Experimental Study of the Influence of Nozzle and Mixing Chamber Dimensions on the Performance of The Ejector

Zuogang Guo[1], Tong Liu[1], Min Xu[1], Yifan Zhou[2], Xinyue Hao[2*], Guangming Chen[2]

1. Electric Power Research Institute, CSG, 510663, Guangdong, Guangzhou
2. Institute of Refrigeration and Cryogenics, Zhejiang University, 310027, Hangzhou, China

Abstract: *The present paper investigates the effect of the primary nozzle and mixing chamber dimensions on the performance of a rectangular ejector using air as the working fluid. The experimental setup is introduced first and the operating conditions and geometrical parameters of the ejector is listed. Five interchangeable nozzles with varied throat diameters and eight mixing chambers with different cross-sectional sizes have been designed in this research. The performance of the ejector equipped with these nozzles and mixing chambers is then experimentally compared. In addition, the influence of different operating conditions on the performance of the ejector equipped with different nozzles and mixing chambers is experimentally examined, and the performance curves of the ejector working in the subcritical and off-design mode are analyzed.*

Key words: *Ejector; Experiment; Dimensions; Performance*

1. Introduction

Ejector uses high-pressure fluid to entrain and pump low-pressure fluid. In a supersonic ejector, the primary fluid is accelerated in a converging-diverging nozzle, resulting in a supersonic fluid that enters the suction chamber. This fluid entrains the secondary fluid and transfer momentum and energy in the mixing chamber. Because of its simple structure and low maintenance cost, ejectors have been widely applied in refrigeration systems [1, 2], fuel cell systems [3, 4] and so on.

Keenan et al. [5] first proposed the one-dimensional mathematical model of a supersonic ejector in 1950. Munday and Bagster [6] extended Keenan's model that the two fluids do not mix immediately at the exit of the primary nozzle but rather at a hypothetical throat (y-y) where the secondary flow approaches critical status. The two streams then mix at constant pressure. Huang [7] further suggested constant-pressure mixing in the constant area mixing chamber of supersonic ejectors and the mixed fluid must go through a normal shock before the diffuser to increase static pressure and reach the designed outlet pressure. For a more accurate evaluation of ejector performance, Zhu et al.[8] proposed a shock circle model that takes into consideration radial velocity distribution at the inlet of the constant-area section. Chen et al. [9]provided a model for determining the ejectors' performance in subcritical mode. Huang et al. [10] recently developed a quasi-two-dimensional ejector model for fuel cell system based on compressible turbulent shear layer development theory which considers ejector's boundary layer, shock train, and mixing layer.

* Corresponding author. Email address: xinyuehao@zju.edu.cn

Furthermore, the compound-choking theory was proposed by Lamberts et al. [11] and Mestue et al. [12] as an explanation for supersonic ejector performance characteristics. They examined the model by experiments and concluded that it performed better in terms of predicting the maximum total mass flow rate. These thermodynamic models for supersonic ejector have played an important role in the design of ejectors and in understanding the internal flow phenomena within the ejectors.

Previous study has discovered that the cross-sectional area of the mixing chamber and the throat area of the primary nozzle have a significant impact on ejector performance. Improvements in ejector performance can be obtained by adjusting these parameters [13, 14]. As a result, it is critical to optimize the ejector's performance by implementing design improvements in the ejector's structure, with the goal of improving internal flow dynamics and ensuring optimal matching between the ejector's structure and operating conditions. Yapici [15] using six configurations of ejector which have a range of area ratio from 6.5 to 11.5 at the compression ratio 2.47 and R-123 as working fluid in an ejector refrigeration system. The experimental results show that the COP of the system rises from 0.29 to 0.41, as the optimum generator temperature increases from 83 to 103 ℃. Thongtip et al. [16] performed experimental research on the impact of the primary nozzle area ratios using R141b as working fluid. They introduced the primary fluid expansion coefficient which is key to indicate the limited range of the working condition, and proper value of the coefficient was determined for various nozzle area ratios. There are also adjustable ejectors [17, 18] which can change its area ratio and nozzle exit position for different operating conditions, and they showed better performance working in off-design mode by choosing the optimal area ratio. It can be observed that the area ratio of the nozzle plays an important role in ejector or system performance.

Some research is also conducted on the influence of the mixing chamber parameters. Chong [19] used both numerical and experimental methods to optimize the mixing chamber design for supersonic ejectors used in boosting natural gas. They claimed that there is an optimal mixing chamber diameter and length to achieve best performance. Fu et al. [20] used numerical methods to study the influences of primary steam nozzle distance and mixing chamber throat diameter on steam ejector performance, and the improvement of the entrainment ratio can reach 25% with the optimization of the mixing chamber diameter. Zhou et al. [21, 22] proposed an innovative way that a compression surface is inserted in the mixing chamber to change the flow area which can improve air ejector performance from their CFD results. The previous literature on the impact of nozzle and mixing chamber structural dimensions on ejector performance is relatively singular, often limited to the variation of a single size. There is less experimental research on the impact brought about by the combination of different sizes of nozzle and mixing chambers. Moreover, both the theoretical and CFD models make necessary assumptions and simplifications for the actual flow process[23, 24], while experiments are the most important means to validate them. Therefore, further verifying theoretical models through experiments and providing more data for the actual design of ejectors still has significant meaning.

This paper presents an experimental study on a rectangular ejector with six primary nozzles which have different throat dimensions and eight mixing chambers which have different geometrical parameters. The experimental setup is first introduced and air is used as the working fluid. Also, the key geometry parameters for designing the supersonic ejector is listed. Secondly,

the experimental rig is described and the experiments were carried out. Lastly, the results of the experiments are discussed and the impact of the geometric parameters and working conditions of the ejector on the performance is evaluated, and the performance curves of the ejector working in the subcritical mode (when outlet pressure exceeds the critical oulet pressure) and off-design mode (when inlet pressure varies from the design condition) are analyzed, providing practical data for further ejector design and theoretical analysis.

2 Experimental Setup

Fig. 1 schematically depicts the experimental setup used in the present study. The main elements of the test facility are a low-pressure air compressor, a low-pressure storage tank, a high-pressure air compressor, a high-pressure storage tank, an adjustable ejector, air filters and measuring devices and valves.

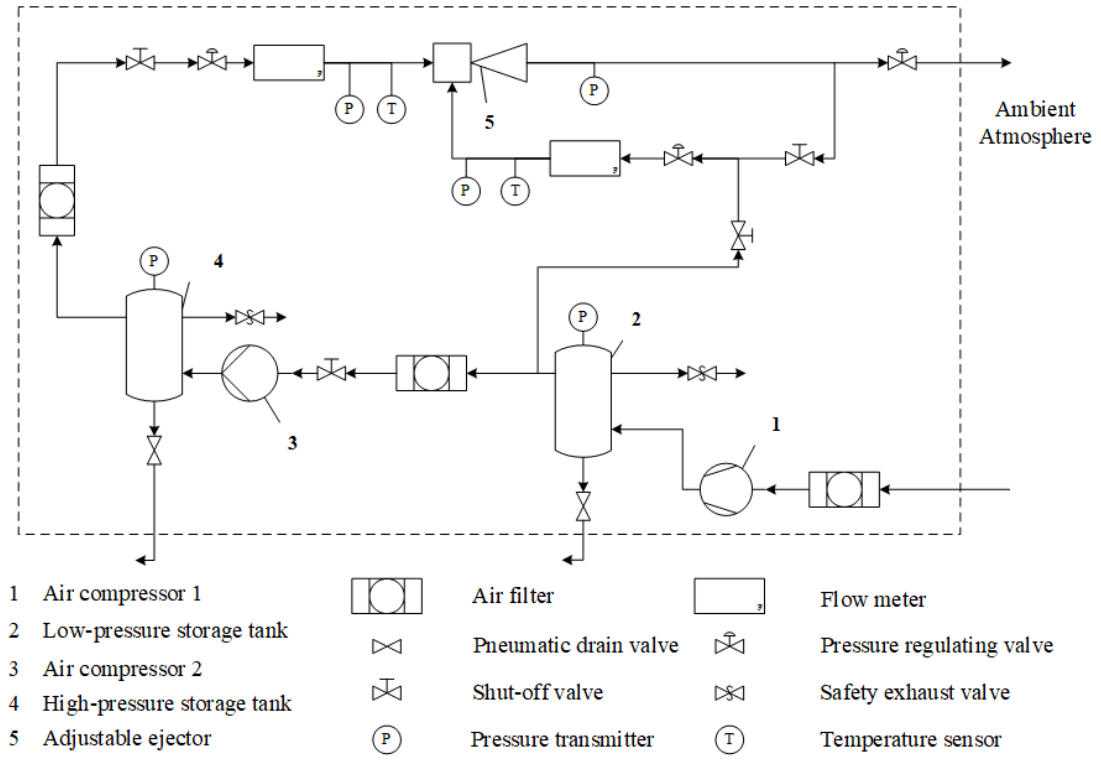

Fig. 1 Schematic diagram of the experimental ejector test rig

The air ejector test rig operates in the following manner. Air from the ambient environment is filtered by an air filter and compressed by the low-pressure air compressor 1 before entering the low-pressure air storage tank. After being filtered once again, the air is further pressurized by the high-pressure air compressor 2 and enters the high-pressure storage tank. The high-pressure air serves as the primary fluid entering the ejector, and a valve is used to control the primary fluid pressure at the ejector inlet. Due to the limited actual power of the air compressor 2, when testing the performance of the ejector under variable working pressure conditions, the gas supply may not be adequate as the gas supply pressure increases. Therefore, exhaust air exiting the ejector is split into two pathways. One passage is entrained by the primary fluid and is pressure-regulated by a pressure lowering valve before entering the ejector. A pressure regulating valve controls the other route, which is a discharge into the atmosphere.

To get simultaneous measurements, the measuring devices were connected to a data

acquisition board. When the board was connected to the computer, the output signals from the measuring devices were sent to the computer, and all readings were automatically monitored and recorded by the computer. Pressure transmitters with 4-20 mA output were used to measure the air pressures. Flowmeters with 4-20 mA output were used to monitor the mass flow rates and air temperatures. All measuring devices, as well as the data collecting system, were calibrated in their measurement range. The flow rate accuracy is 0.25%; the nominal flow rate of the mass flowmeter calculated above is 56 g/s, with a maximum range of 0~84 g/s.

In the experiment, the measurement devices were connected to a data acquisition board to obtain simultaneous readings. Connecting the board to the computer, the output signals from the measurement devices were transferred to the computer and all readings were monitored and also recorded automatically by the computer. The pressures of the air were measured by pressure transmitters with 4–20 mA output. The mass flow rates and temperatures of the air were measured by flow meters with 4–20 mA output. All devices used for measurement were calibrated together with the data acquisition system in their measurement range. The accuracy of mass flow rate is ±0.25% of flow rate; The nominal flow rate of the mass flowmeter calculated above is 56 g/s, with a maximum range of 0~84 g/s. Under design condition, the primary fluid mass flow rate is calculated to be 29.0 g/s, with a variable condition measurement range of 15~58 g/s. The secondary fluid mass flow rate is 16.5 g/s, with a variable condition measurement range of 5~25 g/s. Under design conditions, the relative uncertainty of the entrainment ratio μ of the ejector test system is 1.5%, and the maximum relative uncertainty under variable conditions is 4.4%.

The basic components of the air ejectors are the primary nozzle, suction chamber, mixing chamber, and diffuser. Tab. 1 shows the parameters used when designing the supersonic air ejectors, such as the primary and secondary pressures. The design of structural properties was mostly calculated by the previous ejector model [7, 24], and the essential dimensions of the ejectors used in the experiments are shown in Tab. 2.

Tab. 1. Operating conditions for the ejector

Parameters	Designed Conditions	Variable Conditions
Pressure of primary fluid P_p (kPa)	1000	800-1600
Mass flow rate of primary fluid m_p (g/s)	30	16-60
Pressure of secondary fluid P_s (kPa)	150	Constant
Outlet Pressure P_o (kPa)	250	210-310

Tab. 2. Key geometry parameters of the adjustable ejector

Key Parameters	Value
Area of the nozzle inlet (mm^2)	122
Area of the nozzle exit (mm^2)	19.5
Area of the secondary fluid inlet (mm^2)	555.4
Area of the mixed fluid outlet (mm^2)	820.2
Mixing chamber Length (mm)	100

Diffuser length (mm)	119.8

To investigate the effect of different geometries on ejector performance, this paper considers five primary nozzles with different throat sizes (shown in Fig. 2) and eight mixing chambers with different cross-sectional sizes (shown in Fig. 3), the numbers and specific dimensions of which are listed in **Error! Reference source not found.**. Both numerals (e.g., A2) are used to identify nozzles and mixing chambers in the following discussions.

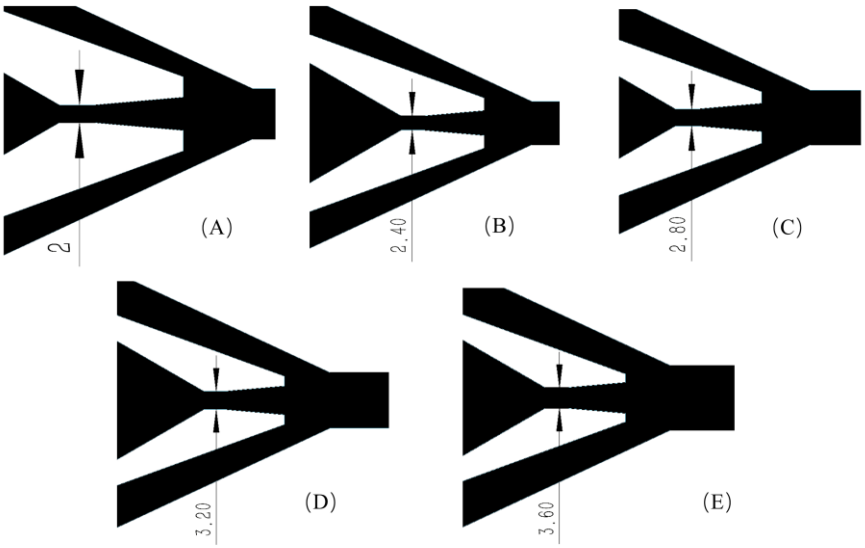

Fig. 2 Dimensions of Nozzle A-E

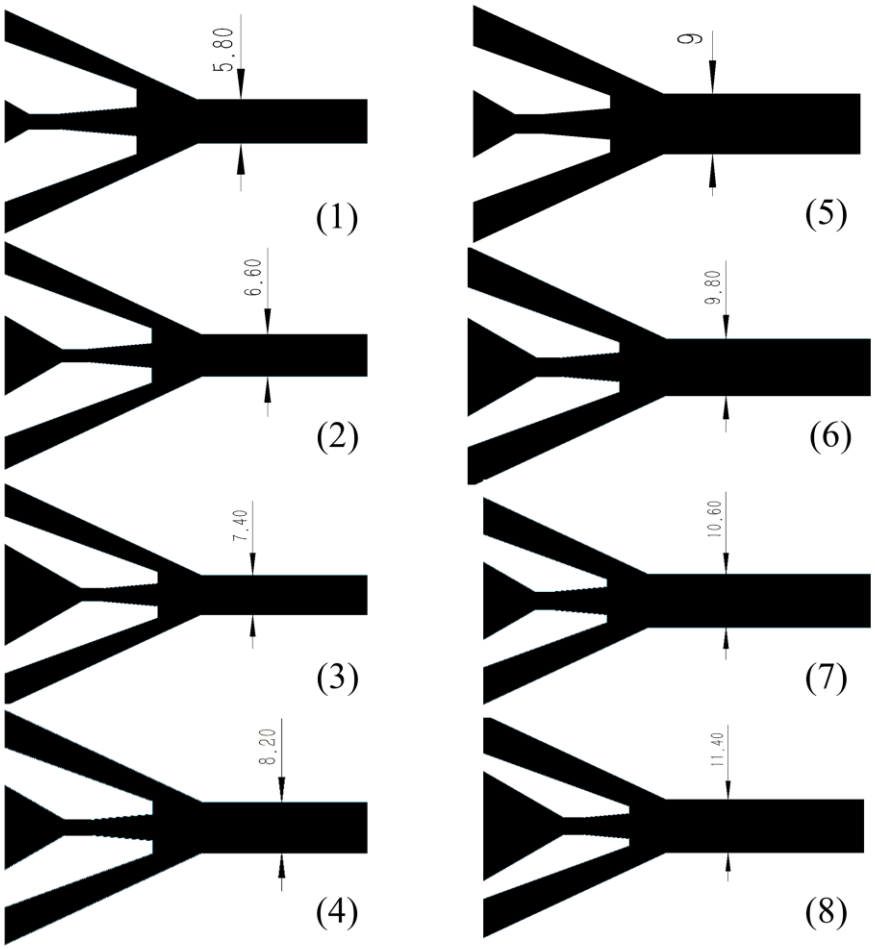

Fig. 3 Dimensions of mixing chamber 1-8

Tab. 3. Numbers and dimensions for the nozzles and mixing chambers

Nozzle number	Nozzle throat dimension	Mixing chamber number	Mixing chamber dimension
A	2.0 mm*4.6 mm	1	9.0 mm*5.8 mm
B	2.4 mm*4.6 mm	2	9.0 mm*6.6 mm
C	2.8 mm*4.6 mm	3	9.0 mm*7.4 mm
D	3.2 mm*4.6 mm	4	9.0 mm*8.2 mm
E	3.6 mm*4.6 mm	5	9.0 mm*9.0 mm
		6	9.0 mm*9.8 mm
		7	9.0 mm*10.6 mm
		8	9.0 mm*11.4 mm

3 Results and discussion

This section mainly focused on the variation of the performance of the ejector for different ejector dimensions and operating conditions. To measure the performance of the ejector,

entrainment ratio, compression ratio or critical outlet pressure are mainly used. The entrainment ratio is used to evaluate the ability of the ejector to entrain the secondary fluid. It is defined as the ratio of the mass flow rate of the secondary fluid to the mass flow rate of the primary fluid, written as:

$$\mu = \frac{m_s}{m_p} = \frac{m_o - m_p}{m_p} \tag{1}$$

The compression ratio is the ratio of the static pressure of the mixed fluid at the ejector outlet to the secondary fluid, which is used to characterize the pressure increase effect that the ejector can provide to the secondary fluid, given by:

$$\lambda = \frac{p_o}{p_s} \tag{2}$$

3.1 Influence of nozzle and mixing chamber dimensions

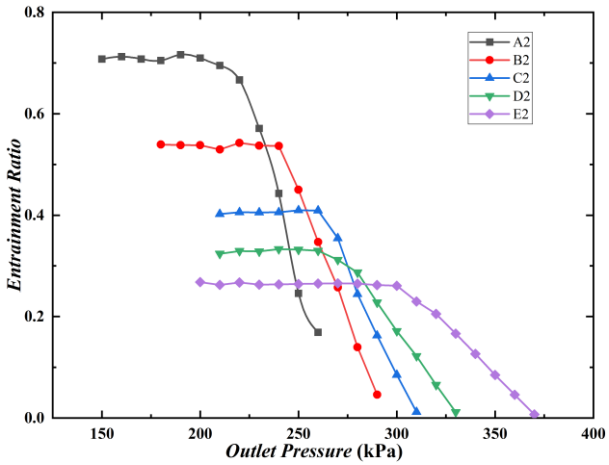

Fig. 4. Variation of the entrainment ratio of the ejector with the outlet pressure for different nozzles

Fig. 4 illustrates the variation of the entrainment ratio of the ejector with the outlet pressure for different nozzle dimensions under designed operating conditions. As can be seen from the figure, when the ejector is equipped with a smaller nozzle (case A2), the maximum entrainment ratio of the ejector increases, and it can obtain better performance at lower outlet back pressure. However, when the outlet back pressure increases, the entrainment ratio decreases significantly. When the ejector is equipped with a larger nozzle (case E2), the maximum entrainment ratio of the ejector is only 0.268, but its critical back pressure is higher than that of the A2, reaching 300 kPa. As the outlet pressure further increases over the critical point, the decline trend of the entrainment ratio is relatively flat.

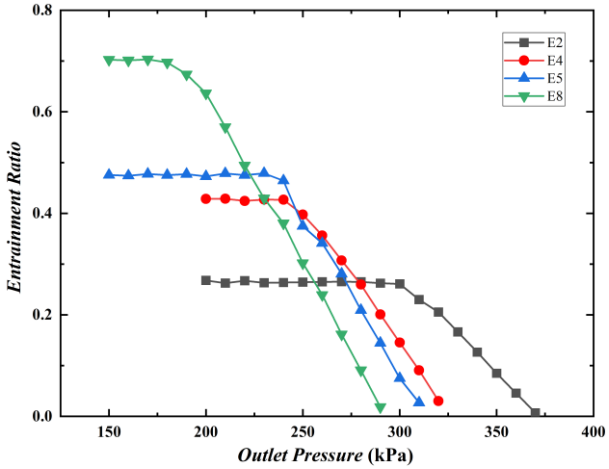

Fig. 5. Variation of the entrainment ratio of the ejector with the outlet pressure for different mixing chambers

Fig. 5 shows variation of the entrainment ratio of the ejector with the outlet pressure for different mixing chamber dimensions under designed conditions. When equipped with a larger mixing chamber (case E8), the ejector can obtain a higher entrainment ratio and a lower critical outlet pressure. When the size of the mixing chamber is reduced, the ejector can work at a higher critical back pressure, and correspondingly, the entrainment ratio also decreases. When the distance of the mixing chamber is adjusted from 6.6 mm (2) to 9.0 mm (5) and 11.4 mm (8) respectively, the critical outlet pressure of the ejector increases from 160 kPa to 250 kPa and 300 kPa, but the entrainment ratio will also decrease from 0.703 to 0.473 and 0.268, respectively. It can be seen that the entrainment ratio and compression ratio usually have two opposite trends, so it is necessary to adjust the ejector structure according to operating conditions.

The ejector tested in this study was designed based on a one-dimensional model[7, 24]. Tab. 4 presents a comparison between the ejector performance predicted by the model and the results of experimental tests. It can be observed that the predicted values of the entrainment ratio are generally lower, while the predicted critical outlet pressures are generally higher. This discrepancy is caused by the fact that the parameters used in the one-dimensional model of the ejector do not match the conditions of the rectangular air ejector. This further illustrates that the experimental work conducted in this study can provide relevant experimental data to help improve relevant theoretical models to predict ejector performance and design ejector parameters.

Tab. 4. Discrepancies between calculated and tested performance

	Calculated μ	Experimental results of μ	Discrepancy	Calculated critical pressure /kPa	Experimental results of critical pressure /kPa	Discrepancy
A2	0.634	0.709	11.8%	272.7	210	-23.0%
B2	0.479	0.538	12.3%	296.6	240	-19.1%
C2	0.368	0.405	10.1%	319.0	260	-18.5%
D2	0.285	0.330	15.8%	340.0	260	-23.5%
E2	0.221	0.262	18.5%	359.6	300	-16.6%
E4	0.346	0.428	23.7%	324.2	240	-26.0%
E5	0.409	0.475	16.1%	310.2	230	-25.9%

E8	0.596	0.702	17.8%	277.9	180	-35.2%

3.2 Variable operating conditions

Besides the nozzle and mixing chamber dimensions mainly discussed in the previous subsection, the primary fluid inlet pressure and the secondary fluid inlet pressure of the ejector have a significant effect on the entrainment ratio and pressure lift ratio of the ejector. In this subsection, the effect of primary and secondary fluid pressure on the performance of ejectors with different nozzles and mixing chambers under off-design conditions is investigated.

3.2.1 Influence of the primary fluid pressure

Fig. 6 shows the variation of the primary and secondary fluid mass flow rate and the entrainment ratio with primary fluid pressure. The graph indicates that the primary fluid flow rate of the ejector is proportional to the primary fluid pressure, and the secondary fluid mass flow rate first increases rapidly and then decreases slowly after the maximum point. This is because as the primary fluid pressure increases, the reverse-flow outlet pressure of the ejector also continues to increase. When the ejector outlet pressure (250 kPa) is smaller than the critical outlet pressure, the ejector transitions from the malfunction mode to the subcritical mode, and the ejector gains the ability to entrain fluid. When the critical back pressure of the ejector further increases to the designed outlet pressure as the primary fluid pressure continues to increase, the ejector operates in the critical mode with optimal entrainment ratio, and the corresponding ejector structure is the optimal ejector structure under this operating condition. However, when the primary fluid pressure further increases, the primary fluid is under-expanded and further expands in the suction chamber, occupying the effective flow area of the secondary fluid, which will cause a decrease in secondary fluid flow rate but also leads to an increase in critical outlet pressure. Therefore, the entrainment ratio of the ejector shows a trend of first rising and then falling.

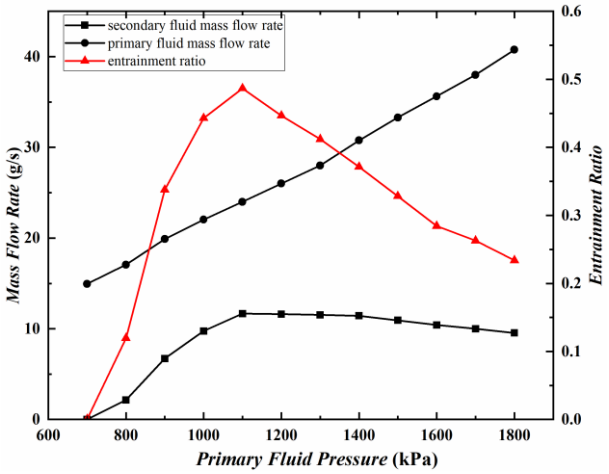

Fig. 6. Variation of mass flow rate and entrainment ratio with the primary fluid pressure for ejector B2

Fig. 7 shows the variation of the entrainment ratio of the ejector with the change of primary fluid pressure when using the nozzle B and different mixing chambers. It can be seen from the figure that the entrainment ratio of the ejector shows a trend of first increasing and then decreasing with the primary fluid pressure. As the area of the mixing chamber increases (adjusted from 1 to

4), the optimal primary fluid pressure for ejector performance is also constantly increasing, and the corresponding entrainment ratio is also constantly increasing, but the minimum primary fluid pressure that allows the ejector to start working is also increasing.

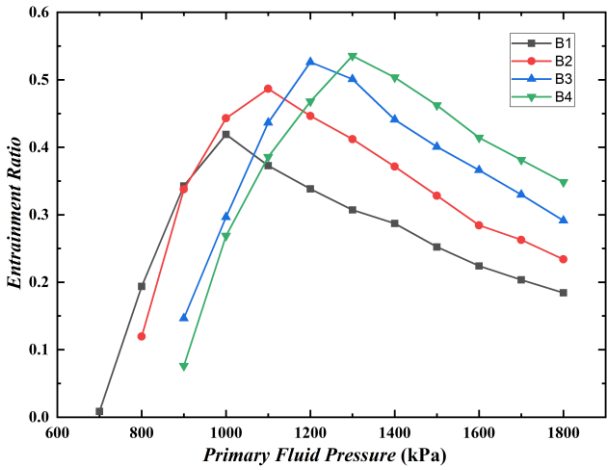

Fig. 7. Variation of entrainment ratio with the primary fluid pressure for nozzle B and different mixing chambers

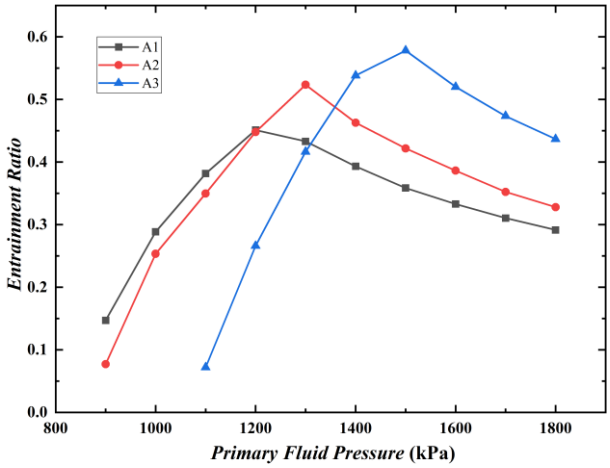

Fig. 8. Variation of entrainment ratio with the primary fluid pressure for nozzle A and different mixing chambers

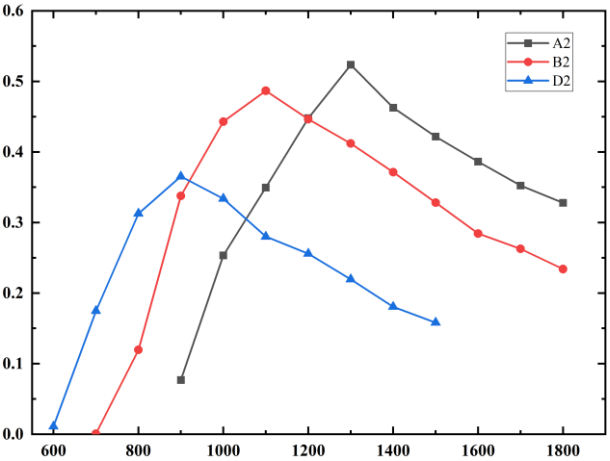

Fig. 9. Variation of entrainment ratio with the primary fluid pressure for mixing chamber 2 and different nozzles

Fig. 8 shows that the variation of the ejector's entrainment ratio when equipped with nozzle A

is dependent on the primary fluid pressure. When equipped with different mixing chamber structures, the ejector's entrainment ratio shows a trend of first increasing and then decreasing with the primary fluid pressure. As the area of the mixing chamber increases (from 5.8 mm to 8.2 mm), the optimal primary fluid pressure for ejector performance is also continuously increasing, which is consistent with previous analysis. For example, when the primary fluid pressure of the ejector is 1200 kPa, mixing chambers 2 and 4 are the optimal mixing chambers corresponding to primary nozzles A and B, and their optimal entrainment ratios are 0.524 and 0.535, respectively.

Fig. 9 shows the variation of the ejector's entrainment ratio with the primary fluid pressure for mixing chamber 2 and different nozzles. Similar to **Error! Reference source not found.**, the entrainment ratio shows a tendency to increase and then decrease with increasing primary fluid pressure. When the size of the mixing chamber remains unchanged, as the nozzle size continues to increase, its area ratio is continuously decreasing, leading to a decrease in optimal primary fluid pressure.

3.2.2 Influence of the secondary fluid pressure

Fig. 10 shows the variation of ejector performance with the change in secondary fluid pressure. As the inlet pressure of the secondary fluid increases, the mass flow rate of the secondary fluid also increases. Since the primary fluid is choked at the throat of the nozzle, its mass flow rate remains basically unchanged, and the entrainment ratio also increases. When the inlet pressure of the secondary fluid is close to the outlet pressure of the ejector at 250 kPa, the entrainment ratio still continues to increase. At this time, the ejector should be more appropriately referred to as a mixer. Even when the pressure of the secondary fluid is greater than the outlet pressure, the mass flow rate of the secondary fluid still maintains an upward trend. After throttling and depressurizing through the ejector, both streams experience a significant drop in temperature. A large amount of water vapour is sprayed out from the ejector outlet.

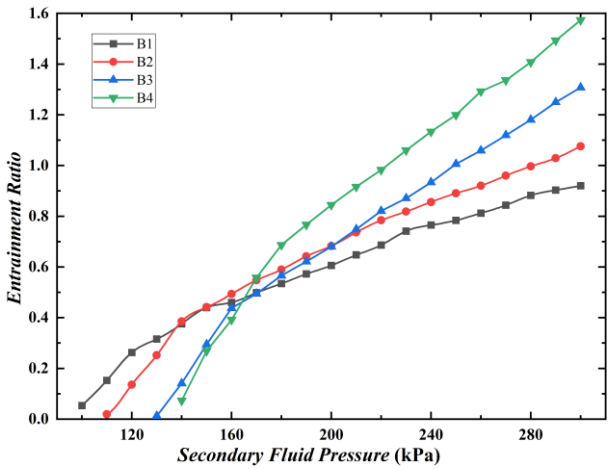

Fig. 10. Variation of entrainment ratio with the secondary fluid pressure for different mixing chambers

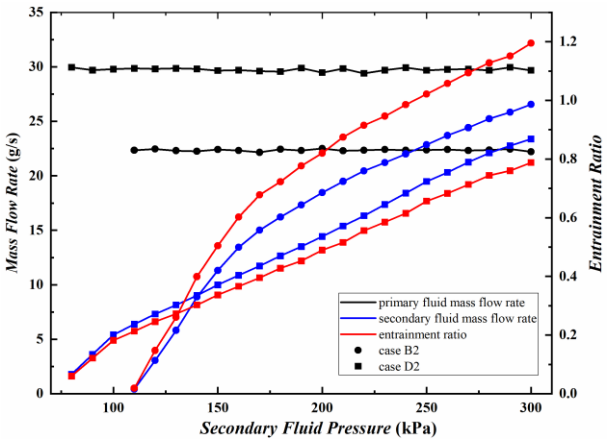

Fig. 11. Variation of ejector performance with the secondary fluid pressure for B2 and D2

A noteworthy phenomenon is that as the secondary fluid pressure increases, the entrainment ratio of the ejector first shows a faster increase, and then slows down. This is due to the fact that when the ejector operates in a single-choking mode, only the primary fluid in the ejector reaches a choking state at the nozzle, and the secondary fluid is not in a choking mode in the mixing chamber. Thus, increasing the pressure of the secondary fluid can quickly increase its mass flow rate that can enter the mixing chamber. When the pressure of the secondary fluid is increased to make the ejector enter the double-choking or critical mode, continuing to increase the pressure of the secondary fluid can improve the ejector's entrainment ratio. However, since the mixing chamber is in a choking state, the increase rate of the entrainment ratio is gentler compared to that in the subcritical mode.

When the mixing chamber area remains constant and a larger nozzle is used, a similar pattern is also presented as shown in Fig. 11. However, the entrainment ratio of the ejector with a smaller nozzle can grow at a larger rate, and its critical back pressure reaches a higher value. As the secondary fluid pressure continues to increase, the entrainment ratio and secondary fluid flow rate of the ejector with a small nozzle can surpass the ejector with a large nozzle. This is because the primary fluid of the ejector in the critical state will occupy the flow area of the secondary fluid. When the ejectors are equipped with a same nozzle but different mixing chamber, an ejector with a smaller mixing chamber can start working at a lower secondary fluid pressure and the entrainment ratio rises more slowly with the increase of the secondary fluid pressure, and it reaches the critical state faster but have a lower entrainment ratio than the ejector with a larger mixing chamber.

4 Conclusions

This paper presents an experimental study on a rectangular ejector using air as the working fluid and investigates the influence of nozzle and mixing chambers dimensions under various operating condition. Five primary nozzles which have different throat dimensions and eight mixing chambers which have different geometrical parameters are designed and tested. The experimental setup and test process are first briefly introduced and the key geometry parameters for designing the supersonic ejector is listed. Then the results of the experiments are discussed and the ejector performance is evaluated.

Results show that:

1. When the ejector is equipped with a smaller nozzle, the entrainment ratio of the ejector in double-choking mode increases, and it can obtain better working performance at lower outlet back pressure. When the ejector is equipped with a larger nozzle, the maximum entrainment ratio of the ejector is only 0.268, but its critical back pressure is higher than that of the A2, reaching 300 kPa.

2. When the ejector is equipped with a smaller mixing chamber size, the entrainment ratio of the ejector in the critical mode decreases, but its critical outlet pressure increases. For example, for the ejector equipped with nozzle E, as the size of the mixing chamber increases from 2 to 8, the critical back pressure decreases from 300 kPa to 160 kPa, but its entrainment ratio increases from 0.268 to 0.703.

3. As the inlet pressure of the primary fluid increases, the mass flow rate of the primary fluid increases, while the mass flow rate of the secondary fluid increases and then decreases; when the size of the nozzle remains constant and the size of the mixing chamber gradually increases, the maximum entrainment ratio increases, and the corresponding optimum primary fluid pressure also increases. When the mixing chamber size is kept constant and the nozzle throat size is gradually increased, the maximum entrainment ratio decreases and the corresponding optimum primary fluid pressure decreases.

4. As the secondary fluid pressure increases, the primary fluid mass flow rate remains constant while the secondary fluid mass flow rate continues to increase. However, the secondary fluid mass flow rate increases faster when the ejector is in the subcritical mode compared to that when the ejector is in the double-choking mode. When the nozzle size is kept constant and the mixing chamber size is gradually increased, the minimum secondary fluid pressure at which the ejector can begin to work increases, and the entrainment ratio increases faster with the secondary fluid pressure. Moreover, the entrainment ratio of the ejector with a larger mixing chamber also increases when working in the double-choking mode. When the mixing chamber size is kept constant and the nozzle throat size gets smaller, the entrainment ratio increases faster with the increase of the secondary fluid pressure. the entrainment ratio of the ejector with smaller nozzle are greater than that with a larger nozzle when working in the double-choking mode.

Acknowledgements

This work is supported financially by the Science & Technology Project of China Southern Power Grid (KYKJXM20210214) and National Natural Science Foundation of Ningbo (NO. 2023J275).

Nomenclature

m	Mass flow rate (kg/s)
P	Pressure (kPa)
Greek symbols	
λ	Compression ratio
μ	Entrainment ratio
Subscripts	
o	Outlet
p	Primary fluid
s	Secondary fluid
Abbreviations	
CFD	Computational fluid dynamics

References

[1] S. Braccio, N. Guillou, N. Le Pierrès, N. Tauveron, H.T. Phan, Mass-flowrate-maximization thermodynamic model and simulation of supersonic real-gas ejectors used in refrigeration systems, Thermal Science and Engineering Progress, 37 January (2023) 101615.

[2] A. Falat, M. Poirier, M. Sorin, A. Teyssedou, Experimental study of the performance of an ejector system using Freon 134a, Experimental Thermal and Fluid Science, 105 (2019) 165-180.

[3] S.T. Soumei Baba, Nariyoshi Kobayashi, Satoshi Hirano, Performance of anodic recirculation by a variable flow ejector for a solid oxide fuel cell system under partial loads, International Journal of Hydrogen Energy, 45 (2020) 10039-10049.

[4] K. Nikiforow, P. Koski, H. Karimaki, J. Ihonen, V. Alopaeus, Designing a hydrogen gas ejector for 5 kW stationary PEMFC system – CFD-modeling and experimental validation, International Journal of Hydrogen Energy, 41 (2016) 14952-14970.

[5] J.H. Keenan, E.P. Neumann, F. Lustwerk, An investigation of ejector design by analysis and experiment, Journal of Applied Mechanics, 17 (1950) 299-309.

[6] J.T. Munday, Bagster DF, A new ejector theory applied to steam jet refrigeration, Ind. Engng Chem., Process Des. Dev., 16 (1977) 442-449.

[7] B.J. Huang, J.M. Chang, C.P. Wang, V.A. Petrenko, A 1-D analysis of ejector performance, International Journal of Refrigeration, 22 (1999) 354-364.

[8] Y. Zhu, W. Cai, C. Wen, Y. Li, Shock circle model for ejector performance evaluation, Energy Conversion and Management, 48 (2007) 2533-2541.

[9] W. Chen, M. Liu, D. Chong, J. Yan, A.B. Little, Y. Bartosiewicz, A 1D model to predict ejector performance at critical and sub-critical operational regimes, International Journal of Refrigeration, 36 (2013) 1750-1761.

[10] Y. Huang, P. Jiang, Y. Zhu, Quasi-two-dimensional ejector model for anode gas recirculation fuel cell systems, Energy Conversion and Management, 262, June (2022) 115674.

[11] O. Lamberts, P. Chatelain, N. Bourgeois, Y. Bartosiewicz, The compound-choking theory as an explanation of the entrainment limitation in supersonic ejectors, Energy, 158 (2018) 524-536.

[12] A. Metsue, R. Debroeyer, S. Poncet, Y. Bartosiewicz, An improved thermodynamic model for supersonic real-gas ejectors using the compound-choking theory, Energy, 238 Part B January (2022) 121856.

[13] J.A. Expósito Carrillo, F.J. Sánchez de La Flor, J.M. Salmerón Lissén, Single-phase ejector geometry optimisation by means of a multi-objective evolutionary algorithm and a surrogate CFD model, Energy, 164 (2018) 46-64.

[14] J. Chen, H. Havtun, B. Palm, Investigation of ejectors in refrigeration system: Optimum performance evaluation and ejector area ratios perspectives, Applied Thermal Engineering, 64 (2014) 182-191.

[15] R. Yapici, H.K. Ersoy, A. Aktoprakoğlu, H.S. Halkacı, O. Yiğit, Experimental determination of the optimum performance of ejector refrigeration system depending on ejector area ratio, International Journal of Refrigeration, 31 (2008) 1183-1189.

[16] T. Thongtip, S. Aphornratana, Impact of primary nozzle area ratio on the performance of ejector refrigeration system, Applied Thermal Engineering, 188 April (2021) 116523.

[17] Z. Chen, H. Zhao, F. Kong, G. Liu, L. Wang, Y. Lai, Synergistic effect of adjustable ejector

structure and operating parameters in solar-driven ejector refrigeration system, Solar Energy, 250 (2023) 295-311.
[18] C. Lin, W. Cai, Y. Li, J. Yan, Y. Hu, K. Giridharan, Numerical investigation of geometry parameters for pressure recovery of an adjustable ejector in multi-evaporator refrigeration system, Applied Thermal Engineering, 61 (2013) 649-656.
[19] D. Chong, J. Yan, G. Wu, J. Liu, Structural optimization and experimental investigation of supersonic ejectors for boosting low pressure natural gas, Applied Thermal Engineering, 29 (2009) 2799-2807.
[20] W. Fu, Z. Liu, Y. Li, H. Wu, Y. Tang, Numerical study for the influences of primary steam nozzle distance and mixing chamber throat diameter on steam ejector performance, International Journal of Thermal Sciences, 132 (2018) 509-516.
[21] Y. Zhou, G. Chen, X. Hao, N. Gao, O. Volovyk, A theoretical model for performance evaluation of a novel configuration of supersonic ejectors, Applied Thermal Engineering, 231 August (2023) 120867.
[22] Y. Zhou, G. Chen, X. Hao, N. Gao, O. Volovyk, Working mechanism and characteristics analysis of a novel configuration of a supersonic ejector, Energy, 278 Part B 1 September (2023). 128010
[23] B.M. Tashtoush, M.d.A. Al-Nimr, M.A. Khasawneh, A comprehensive review of ejector design, performance, and applications, Applied Energy, 240 (2019) 138-172.
[24] V. Kumar, G. Sachdeva, 1-D model for finding geometry of a single phase ejector, Energy, 165 (2018) 75-92.

Submitted: 13.02.2024
Revised: 25.05.2024
Accepted: 06.06.2024